IOPscience iopscience.iop.org

Home Search Collections Journals About Contact us My IOPscience

Will silicon be the photonic material of the third millenium?

This article has been downloaded from IOPscience. Please scroll down to see the full text article.

2003 J. Phys.: Condens. Matter 15 R1169

(http://iopscience.iop.org/0953-8984/15/26/201)

View the table of contents for this issue, or go to the journal homepage for more

Download details:
IP Address: 171.66.16.121
The article was downloaded on 19/05/2010 at 12:09

Please note that terms and conditions apply.

INSTITUTE OF PHYSICS PUBLISHING JOURNAL OF PHYSICS: CONDENSED MATTER

J. Phys.: Condens. Matter **15** (2003) R1169–R1196 PII: S0953-8984(03)39709-7

TOPICAL REVIEW

Will silicon be the photonic material of the third millenium?*

L Pavesi

INFM and Dipartimento di Fisica, Universita' di Trento, Via Sommarive 14, 38050-Povo Trento, Italy

E-mail: pavesi@science.unitn.it

Received 24 April 2003
Published 20 June 2003
Online at stacks.iop.org/JPhysCM/15/R1169

Abstract
Silicon microphotonics, a technology which merges photonics and silicon microelectronic components, is rapidly evolving. Many different fields of application are emerging: transceiver modules for optical communication systems, optical bus systems for ULSI circuits, I/O stages for SOC, displays, ... In this review I will give a brief motivation for silicon microphotonics and try to give the state-of-the-art of this technology. The ingredient still lacking is the silicon laser: a review of the various approaches will be presented. Finally, I will try to draw some conclusions where silicon is predicted to be the material to achieve a full integration of electronic and optical devices.

(Some figures in this article are in colour only in the electronic version)

Contents

1. Why silicon photonics? 1170
2. Silicon photonics 1172
   2.1. Silicon based waveguides 1172
   2.2. Detectors 1173
   2.3. Other photonics components 1174
   2.4. Silicon photonic integrated circuits 1174
3. Silicon laser 1176
   3.1. Bulk silicon 1177
   3.2. Silicon nanocrystals 1180
   3.3. Er coupled silicon nanocrystals 1186
   3.4. Si/Ge quantum cascade structures 1188
   3.5. THz emission 1191

* This review is based on the books *Light Emitting Silicon for Microphotonics* by S Ossicini, L Pavesi and F Priolo *(Springer Tracts in Modern Physics)*, at press, and *Towards the First Silicon Laser* edited by L Pavesi, S Gaponenko and L Dal Negro *(NATO Science Series II)* vol 93 (Dordrecht: Kluwer), 2003.

0953-8984/03/261169+28$30.00 © 2003 IOP Publishing Ltd Printed in the UK

4. Conclusion 1193
Acknowledgments 1193
References 1193

1. Why silicon photonics?

The big success of today's microelectronic industry is based on various factors, among others

- the presence of a single material, silicon, which is widely available, can be purified to an unprecedented level, is easy to handle and to manufacture and shows very good thermal and mechanical properties which render the processing of devices based on it easy [1],
- the availability of a natural oxide of silicon, SiO_2, which effectively passivates the surface of silicon, is an excellent insulator, is an effective diffusion barrier and has a very high etching selectivity with respect to Si,
- the presence of a single dominating processing technology, CMOS, which accounts for more than 95% of the whole market of semiconductor chips [2],
- the possibility to integrate more and more devices, 55 000 000 transistors in PENTIUM® 4 (figure 1), on larger and larger wafers (300 mm process and 400 mm research) with a single transistor size which is decreasing (gate lengths of 180 nm are in production while 15 nm have been demonstrated) [3], yielding a significant reduction in cost per bit,
- the ability of the silicon industry to face improvements when the technology is hitting the so-called red brick wall, e.g. the use of SiGe for high frequency operation and the introduction of low k-materials and of Cu to reduce RC delays,
- an accepted common roadmap which is dictating the technology evolution for processes, architectures or equipment [3] and
- the presence of big companies which define standards and trends (almost 90% of the market is shared by ten companies).

All these factors have rendered the microelectronics industry very successful. However, in recent years some concerns about the evolution of this industry have been raised which seem related to fundamental materials and processing aspects [4]. An important example is related to the limitations of the operating speed of microelectronic devices due to the interconnect [5]. Figure 2 shows the signal delay as a function of the generation of transistors [6]. For gate length shorter than 200 nm, a situation is reached where the delay is no longer dictated by the gate switching time but by the wiring delay. In addition, as the integration is progressing the length of the interconnects on a single chip is getting longer and longer. Nowadays chips have total interconnection length per unit area of the chip of some 5 km cm^{-2} with a chip area of 450 mm^2 while in ten years from now these lengths will become 20 km cm^{-2} for a chip area of 800 mm^2. The problem is not only related to the length of the interconnects but also to the complexity of their architecture. Nowadays, there are six layers of metal levels (figure 3), while in ten years from now there will be more than 12. All these facts introduce problems related to the delay in signal propagation causing RC coupling, signal latency, signal cross-talk and RL delays due to the reduction in dimension and increase in density of the metal line. A possible solution to these problems is looked for in optics [7]: the use of optical interconnects. Nowadays, optical interconnects through optical fibres and III–V laser sources are already used to connect different computers. It is predicted that optical interconnects will be used to connect computer boards in five years, while the use of optical interconnects within the chip is being investigated and will possibly be realized in 10–15 years from now [8]. Optical interconnects are one of the main motivations to look for silicon photonics. But this is not the only one. Photonics has seen a big development in recent years at the request of the communication market, where more and

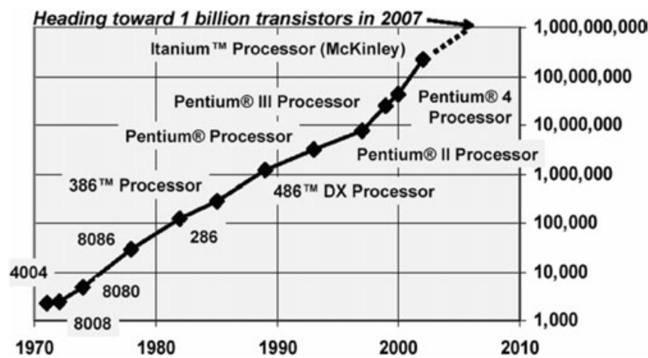

Figure 1. Evolution of the number of transistors in a single CPU (central processing unit) versus the year. This graph is based on the Intel CPU [6].

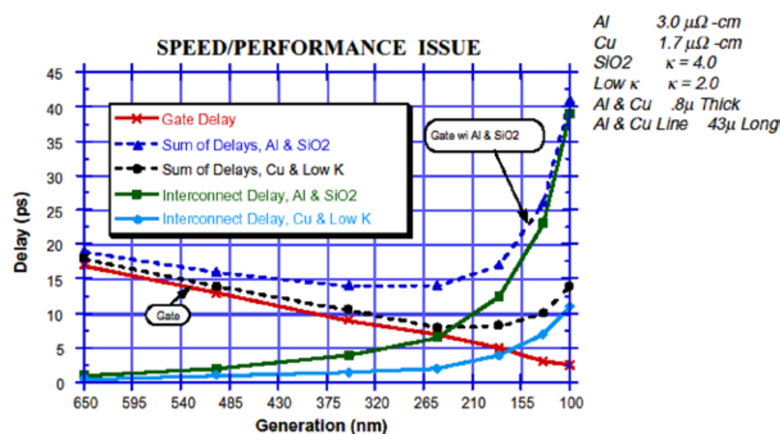

Figure 2. Calculated gate delay and wire delay as a function of the minimum feature size (device generation). From SIA Roadmap 1997 [3]. Interconnections and signal integrity, DAC tutorial. *38th Design Automation Conf.* ©2001 (www.amanogawa.com/epep2000/files/jose1.pdf).

more information has to be sent at higher and higher speed. Nowadays, the capacity of optical communication on long hauls is reaching some Tb/s^{-1} over thousands of kilometres. And all these are thanks to the progress in optical fibre fabrication, the use of DWDM, of EDFA and Raman amplifiers, modulators and single frequency lasers.

If one compares the photonic industry with microelectronics today one can see many differences.

(1) A variety of different materials is used: InP as substrate for source development, silica as material for fibres, lithium niobate for modulators, other materials for DWDM and EDFA and so on.
(2) No single material or single technology is leading the market. Some convergence is appearing towards the use of InP as the substrate material to integrate different optical functions.
(3) The industry is characterized by many different small companies which are specialized in specific devices: lasers, modulators etc. No big companies are dominating at present.
(4) The production technology is still very primitive. Chip scale integration of optical components, which enables low cost and high reproducibility, is not yet achieved. Neither

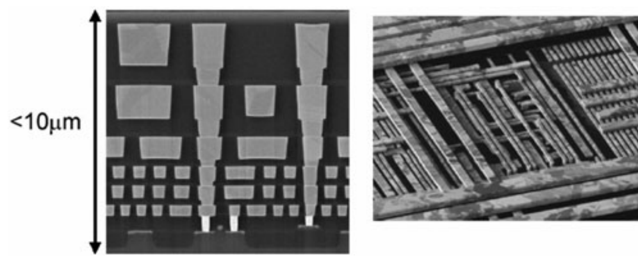

Figure 3. An example of the complexity of the metal interconnects in today's chip. Left chip cross-section: most of the chip is occupied by metal interconnect layers. Right: the complexity of the architecture of the metal line. From a talk by Joise Maiz at the Spanish Microsystems Research Centre (CMIC) on 14 June 2002 (http://www.intel.com/research/silicon/CMIC_2002_Jose_Maiz.htm).

standardization of processes nor packaging of optical components, which is inherent for mass production and repeatability, are present.

(5) Roadmaps to dictate and forecast the evolution of photonics are only now being elaborated [9].

It is commonly accepted that the industrial model of microelectronics if applied to photonics will be a booster to the development and implementation of photonics. To describe this new technology the term of microphotonics has been proposed [11]. All the big players of microlectronics have aggressive programmes to develop microphotonics, mostly based on silicon [10].

The aim of this review is to try to give the state-of-the-art on the development of silicon photonics with the aim of settling the status and trying to weigh up whether silicon can be used as *the* photonics material. For this reason, all the different components are briefly reviewed (section 2) with a special emphasis on the subject which is at the forefront of today's discussion: the route to a silicon laser (section 3). The selection of the various experimental data is not intended to be exhaustive but simply representative of some of the more successful devices and integration schemes which have been reported. I apologize in advance to all those authors whose work I am not referring to.

2. Silicon photonics

It was predicted in the early 1990s that silicon based optoelectronics would be a reality before the end of the century [12, 13]. Indeed, all the basic components have already been demonstrated [14], except for a silicon laser.

2.1. Silicon based waveguides

The first essential component in silicon microphotonics is the medium through which light propagates: the waveguide. This has to be silicon compatible and should withstand normal microelectronics processing. Critical parameters are the refractive index of the core material, its electro-optical effects, the optical losses and the transparency region. To realize low loss optical waveguides, various approaches have been followed [15]: low dielectric mismatch structures (e.g. doped silica [16], silicon nitride [17] or silicon oxynitride on oxide [18], or differently doped silicon [19]) or high dielectric mismatch structures (e.g. silicon on oxide [11]). Low loss silica waveguides are characterized by large dimensions (see figure 4), typically 50 μm of thickness, due to the low refractive index mismatch ($\Delta n = 0.1$–0.75%). Silica waveguides

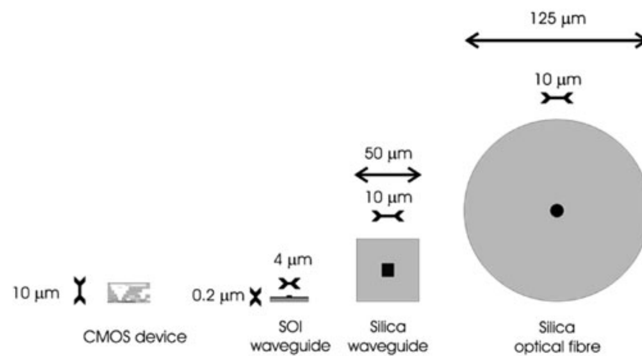

Figure 4. Comparison of the cross-sections of a CMOS chip, a typical SOI waveguide, a typical silica waveguide and a silica mono-mode optical fibre.

have a large mode spatial extent and, thus, are interesting for coupling with optical fibres but not for integration into/within electronic circuits because of a significant difference in sizes. The large waveguide size also prevents the integration of a large number of optical components in a single chip. Similar problems exist for silicon on silicon waveguides where the index difference is obtained by varying the doping density [19]. Silicon on silicon waveguides are very effective for realizing free-carrier injection active devices (e.g. modulators) as well as fast thermo-optic switches thanks to the high thermal conductivity of silicon. A major problem with these waveguides is the large free-carrier absorption which causes optical losses of some dB cm^{-1} for single-mode waveguides at 1.55 μm. Silicon nitride based waveguides [17] and silicon oxynitride waveguides [18] show losses at 633 nm lower than 0.5 dB^{-1} and bending radii of less than 200 μm. The nitride based waveguides are extremely flexible with respect to the wavelength of the signal light: both visible and IR.

At the other extreme, silicon on insulator (SOI) or polysilicon based waveguides allow for a large refractive index mismatch and, hence, for small size waveguides in the sub-micrometre range. This allows a large number of optical components to be integrated within a small area. Optical losses as low as 0.1 dB cm^{-1} at 1.55 μm have been reported for channel waveguides in SOI (optical mode cross-section 0.2×4 μm^2) [20]. Ideal for on-chip transmission, SOI waveguides have coupling problems with silica optical fibre due to both the large size difference and the different optical impedance of the two systems (figure 4). Various techniques have been proposed to solve these problems, among which are adiabatic tapers, V-grooves and grating couplers (figure 5) [21, 22]. Large single-mode stripe loaded waveguides on SOI can be achieved provided that the stripe and the slab are both made of silicon [23]. This SOI system provides low loss waveguides (<0.2 dB cm^{-1}) with single-mode operation with large rib structures (optical mode cross-section 4.5×4 μm^2) and low birefringence ($<10^{-3}$). Appropriate geometry with the use of an asymmetric waveguide allows bend radii as short as 0.1 mm [24]. A number of photonic components in SOI have been demonstrated [23] and commercialized [24]: directional couplers, dense WDM arrayed waveguide grating, Mach–Zehnder filters, star couplers, ...

2.2. Detectors

The optical signal is converted into an electrical signal by using silicon based photodetectors. Detectors for silicon photonics are based on three different approaches [25]: silicon photoreceivers for $\lambda < 1.1$ μm, hybrid systems (mostly III–V on Si) and heterostructure based systems. High speed (up to 8 Gb s^{-1}) monolithically integrated silicon photoreceivers

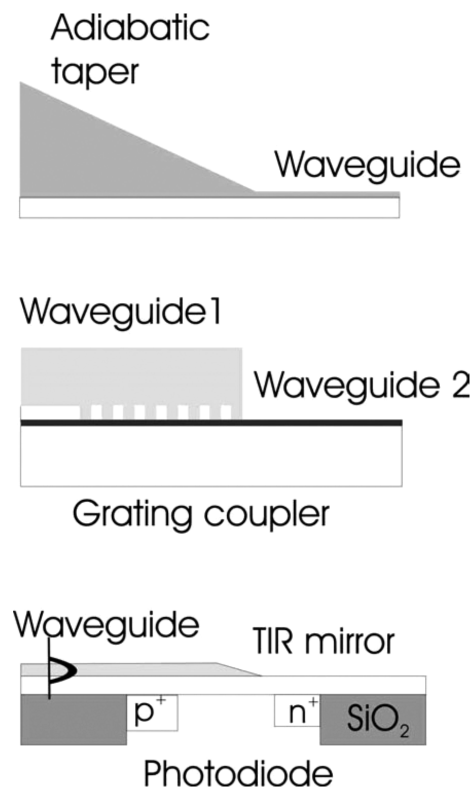

Figure 5. Various schemes to couple the light from a fibre into a waveguide by using an adiabatic taper or a grating coupler, or from a waveguide into a photodiode by using a curved TIR (total internal reflection) mirror.

at 850 nm have been fabricated by using 130 nm CMOS technology on a SOI wafer [26]. Other recent results confirm the ability of silicon integrated photoreceivers to detect signals with a high responsivity of 0.46 A W^{-1} at 3.3 V for 845 nm light and 2.5 Gb s^{-1} data rate [27]. The heterostructure approach is mainly based on the heterogrowth of Ge rich SiGe alloys: Ge-on-Si photodetectors have been reported with a responsivity of 0.89 A W^{-1} at 1.3 μm and 50 ps response time [28]. 1% quantum efficiency at 1.55 μm in an MSM (metal–semiconductor–metal) detector based on a Si/SiGe superlattice shows that promising developments are possible [29]. Similarly a waveguide photodetector with Ge/Si self-assembled islands shows responsivities of 0.25 mW at 1.55 μm with zero bias [30].

2.3. Other photonics components

Almost all the other photonics components have been demonstrated in silicon microphotonics [13, 25]. Optical modulators, optical routers and optical switching systems have been all integrated into silicon waveguides [31]. Discussion of a series of photonics components realized with SOI waveguides is given in [23] which includes plasma dispersion effect based active gratings, evanescent waveguide coupled silicon–germanium based photodetectors and Bragg cavity resonant photodetectors.

2.4. Silicon photonic integrated circuits

Based on the technologies reported in the previous sections, various demonstrations of photonic integrated circuits based on silicon have been reported. Here we discuss some examples.

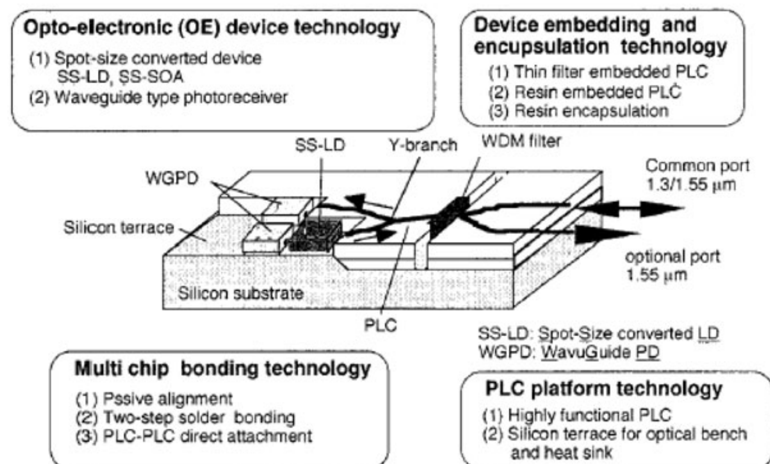

Figure 6. Example of the various devices that can be integrated on a silica based lightwave circuit. SS-LD stands for laser diode, WGPD stands for photodetectors (from [32]).

Hybrid integration of active components and silica-based planar lightwave circuits provides a full scheme for photonic component integration within a chip [32]. Passive components are realized by using silica waveguides while active components are hybridized within the silica (see figure 6). Active components (laser diodes, semiconductor optical amplifiers and photodiodes) are flip-chip bonded on silicon terraces where the optical waveguides are also formed. By using this approach, various photonic components have been integrated such as multi-wavelength light sources, optical wavelength selectors, wavelength converters, all optical time-division multiplexers etc [32]. Foreseen applications are WDM transceiver modules for fibre-to-the-home application.

A full integrated optical system based on silicon oxynitride waveguides, silicon photodetectors and CMOS transimpedance amplifiers has been realized [18]. Coupling of visible radiation to a silicon photodetector can be achieved by using mirrors at the end of the waveguide (figure 5). These are obtained by etching the end of the waveguide with an angle so that the light is reflected at almost 90° into the underlying photodetector. A schematic diagram of the cross-section of the device is shown in figure 7.

Commercial systems for the access network telecom market have been realized by using SOI waveguides and the silicon optical bench approach to interface the waveguides with both III–V laser sources and III–V photodetectors. The silicon optical bench (SOB) is a technology where the silicon wafer is used as a substrate (*optical bench*) where the various optical components are inserted by micromachining suitable lodging. In [24], lasers and photodetectors are stuck into etched holes in silicon and bump soldered in place. The system operates at 1.55 μm with a typical bit rate of 155 Mb s^{-1} [24]. A further advantage of the use of a large optical mode waveguide is the ease of interfacing to single-mode optical fibre. In the approach of [24], these are located in V-grooves etched into silicon.

A fully integrated system working at 1.55 μm has been demonstrated based on silicon waveguides with very small optical mode (cross-section $0.5 \times 0.2\ \mu$m^2) which allows extremely small turn radii (1 μm) [11]. In this way a large number of optical components can be integrated on a small surface ($\approx$10 000 components cm^{-2}). Detectors are integrated within silicon by using Ge hetero-growth on silicon itself. Responsivity of 250 mA W^{-1} at 1.55 μm and response times shorter than 0.8 ns have been achieved [28]. A scheme for an optical clock distribution

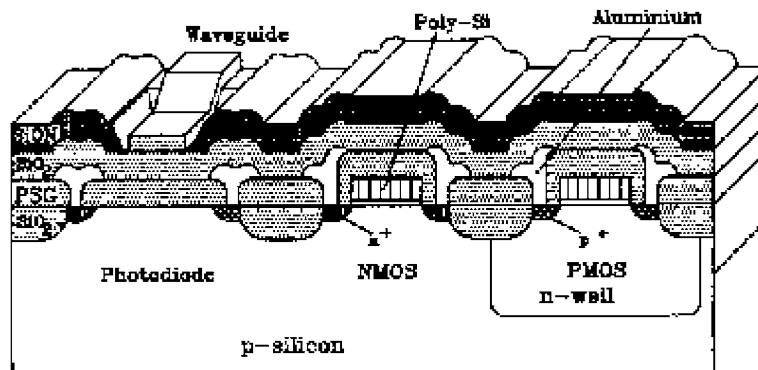

Figure 7. Cross section of an integrated device with a photodiode (PD) (left), the waveguide coupled to the PD by the TIR mirror and an amplifier stage realized with CMOS technology (from [18]).

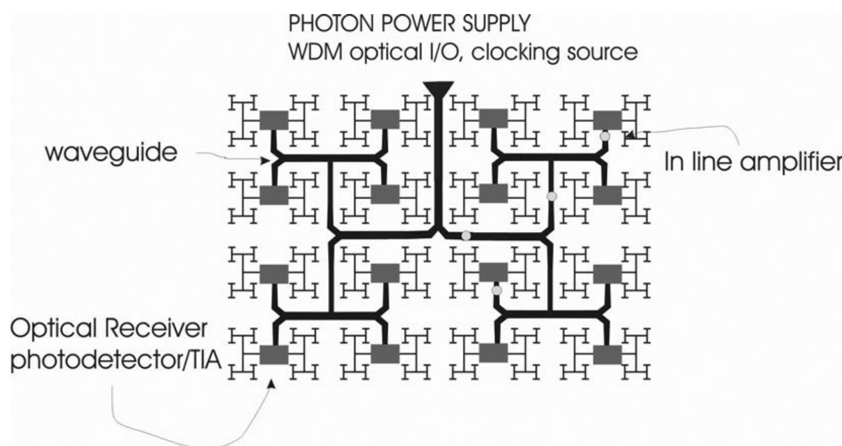

Figure 8. Scheme for an integrated optical circuit to distribute the clock signal on a chip (from [33]).

within integrated circuits based on this approach is shown in figure 8 [33]. Here the laser source is external to the chip and acts as a *photon battery* similarly to usual batteries for electrons.

A realistic bidirectional optical bus architecture for clock distribution on a Cray T-90 supercomputer board based on polyimide waveguides (loss of 0.21 dB cm^{-1} at 850 nm), a GaAs VCSEL and silicon MSM photodetectors has been investigated [34]. By using 45° TIR (total internal reflection) mirror coupling efficiencies as high as 100% among the sources or the detectors and the waveguides have been demonstrated. Examples of the connection scheme are shown in figure 9.

3. Silicon laser

To achieve monolithically integrated silicon microphotonics, the main limitation is the lack of any practical Si-based light sources: either efficient light emitting diodes (LEDs) or Si lasers. A laser is preferred as incoherent emission is probably not sufficient for dense, high speed interconnects mostly because of the basic optical inefficiencies in focusing incoherent light. A laser is ideal for optical interconnects, or more generally speaking, for silicon

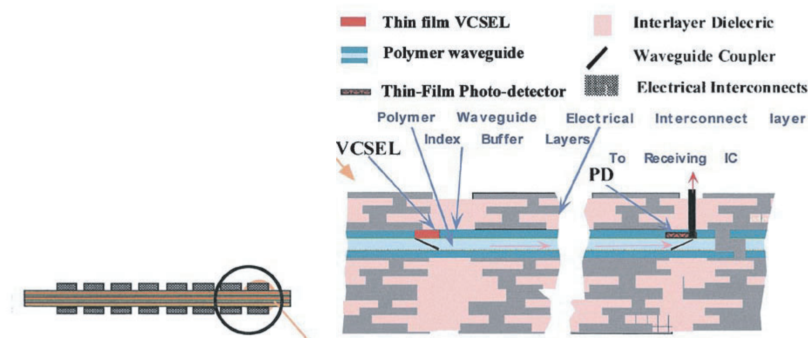

Figure 9. The optical interconnect scheme proposed in [34] for a supercomputer board: left, schematic diagram of the side view of the vertical integration layers; right, details of the schematic diagram (from [34]).

microphotonics. Unfortunately, today, the only viable solution is the hybrid approach where III–V semiconductor lasers are grown, bonded or connected to silicon photonic integrated circuits. To have a silicon laser, or in general a laser, one needs three key ingredients:

(i) an active material which should be luminescent in the region of interest and which should be also able to amplify light,
(ii) an optical cavity into which the active material should be placed to provide the positive optical feedback and
(iii) a suitable and efficient pumping scheme to achieve and sustain the laser action; for integration purposes the pumping mechanism is preferable via electrical injection.

Silicon is an indirect bandgap material; light emission is a phonon-mediated process with low probability (spontaneous recombination lifetimes in the milliseconds range) [35]. In standard bulk silicon, competitive non-radiative recombination rates are much higher than the radiative ones and most of the excited e–h pairs recombine non-radiatively. This yields very low internal quantum efficiency ($\eta_i \approx 10^{-6}$) for bulk silicon luminescence. In addition, fast non-radiative processes such as *Auger* or *free-carrier* absorption severely prevent population inversion for silicon optical transitions at the high pumping rates needed to achieve optical amplification. Despite all this, during the 1990s many different strategies have been employed to overcome these materials limitations [35]. The most successful ones are based on the exploitation of low dimensional silicon where silicon is nanostructured and hence the electronic properties of free carriers are modified by quantum confinement effects [13]. A steady improvement in silicon LED performances has been achieved and silicon LEDs are now within the strict market requirements [36]. In addition, many breakthroughs have been recently demonstrated showing that this field is very active and still promising [36–40]. Figure 10 shows a schematic sketch of the various strategies that are currently followed to build a silicon laser [41]. They differ both for spectral region of emission and for the physics behind. In the following, I will review all these approaches and try to weigh them up.

3.1. Bulk silicon

Silicon is an indirect bandgap material, thus the probability for a radiative transition is very low. This is reflected in very long times for radiative recombinations. Due to these long radiative lifetimes, excited free carriers have large probabilities of finding non-radiative recombination

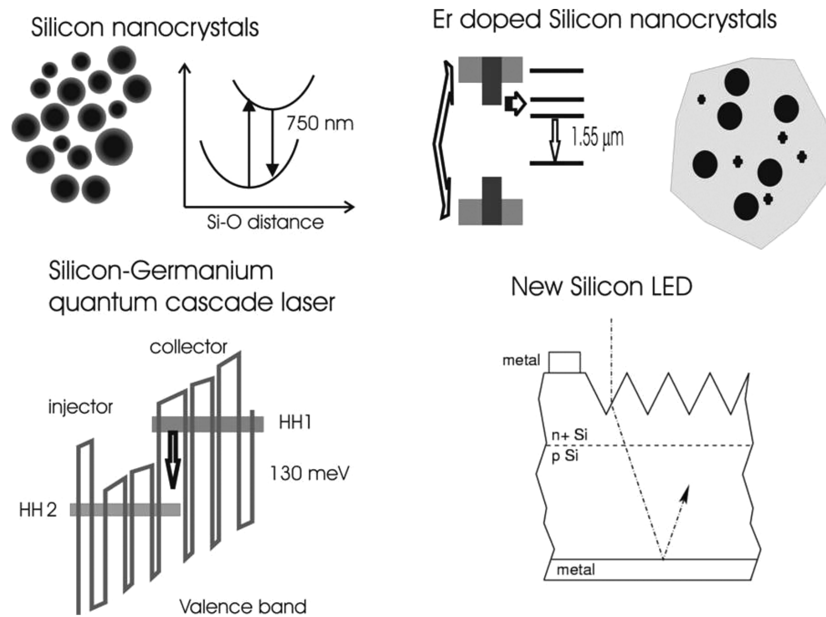

Figure 10. Various approaches proposed to realize a silicon laser.

centres and recombining non-radiatively. Room temperature emission in bulk silicon with high efficiency has only been observed in ultra-pure silicon with the surface passivated by a native oxide where excited carrier lifetimes are dominated by radiative recombination. Extremely slow recombination rates are possible with high efficiency if one is able to reduce to a minimum the competing non-radiative recombinations. This idea to increase the quantum efficiency of Si has been followed by two different approaches to develop Si based light emitting diodes [36, 42].

The first approach is based on the results achieved in high efficiency solar cells and on the consideration that, within thermodynamic arguments, absorption and emission are two reciprocal processes [36]. At first the non-radiative rates are reduced by using

(1) high-quality intrinsic Si substrates, float zone (FZ) being preferred over Czochralski (CZ),
(2) passivation of surfaces by high quality thermal oxide, in order to reduce surface recombination,
(3) small metal areas and
(4) limiting the high doping regions to contact areas, in order to reduce the Shockley–Read–Hall recombinations in the junction region.

Then, the parasitic absorption of photons once they have been generated is reduced to a minimum. For example, the reabsorption can be minimized by keeping the doping level to moderate values, such as $\sim 1.4 \times 10^{16}$ cm^{-3}. Finally, the extraction efficiency of light from bulk silicon can be enhanced by suitably texturizing the Si surface. The final device structure is shown in figure 11. Green *et al* [36] report the highest power efficiency to date for Si based LEDs, approaching 1%. Electroluminescence (EL) spectra of these devices (figure 12) are typical for band-to-band recombinations in silicon. In addition, a fully integrated opto-coupler device (LED coupled to a photodetector) was also demonstrated on the basis of this technology [43].

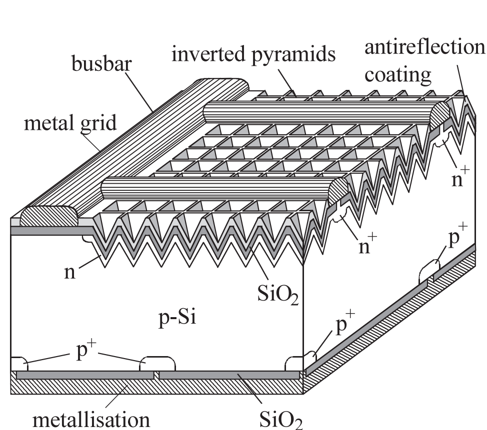

Figure 11. Design of the textured Si light emitting device after [36].

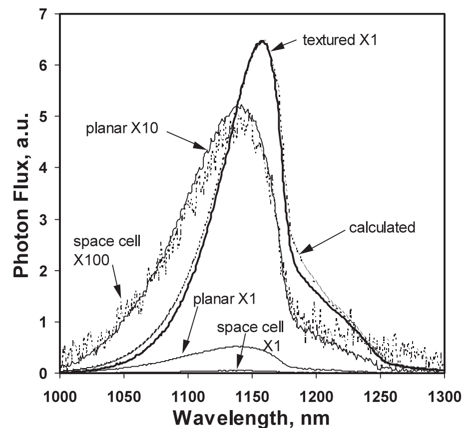

Figure 12. EL spectra for textured, planar and baseline space cell diodes under 130 mA bias current at 298 K (diode area 4 cm^2). Calculated values assume a rear reflectance of 96% (after [36]).

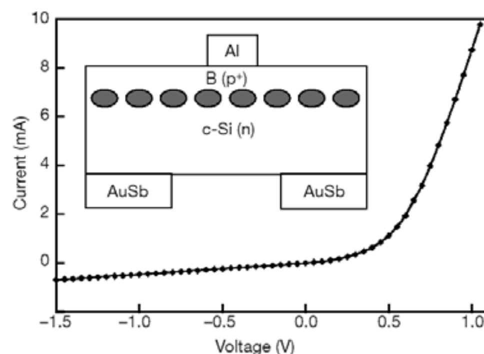

Figure 13. Current–voltage characteristics for the dislocation loop LED measured at room temperature. Inset: a schematic diagram of the LED where the grey circles evidence the region rich in dislocation loops (after [42]).

The main drawbacks of this approach for an integrated laser or light emitting diode are the following:

(i) the need for both high purity (low doping concentration) and surface texturing renders the device processing not compatible with standard CMOS processing;
(ii) the strong and fast free-carrier absorption typical of bulk Si, that can prohibit reaching the condition for population inversion, is not addressed [44];
(iii) the suitable integration of the active bulk Si into an optical cavity to achieve the required optical feedback to sustain a laser action can be a problem;
(iv) the modulation speed of the device can be limited by the long lifetime of the excited carriers (milliseconds) and by the need for a large optical cavity.

A somewhat different approach was reported in [42]; see figure 13. The idea was again a reduction of the non-radiative channels by exploiting the strain produced by localized dislocation loops to form energy barriers for carrier diffusion. Dislocations form potential pockets close to the junction which block the carriers and enhance radiative decay by localizing

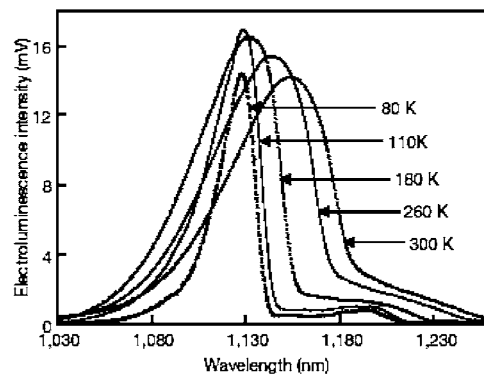

Figure 14. EL spectra against wavelength at various temperatures. The device was operated at a forward current of 50 mA for all temperatures (after [42]).

them in defect-free regions. The size of dislocation loops was in the range of 100 nm, i.e. not enough to cause a quantum confinement of the carriers, and the loop distances were of the order of 20 nm. Free carriers injected through the top electrode are not able to diffuse away and then are constrained to recombine in the near junction region. The onset of the EL at the band edge was observed as the diode turns on under forward bias. No EL was observed under reverse bias. An ultimate external quantum efficiency of about 1% is claimed for these LEDs. The EL spectrum does not present significant differences in lineshape and peak position compared to that of bulk Si (figure 14). A remarkable feature of this device is the high injection efficiency into the confined regions. This is due to the lack of quantum effects. In fact, since the density of states in the active zone is large (comparable to the bulk value), it is not a limiting factor for the free-carrier injection, in contrast to quantum confined structures. On the other hand, injection is also smooth because there is no wide bandgap material as confining barrier. Although not explained, this device has the additional and interesting feature of increasing the efficiency with temperature. The positive role of dislocation loops in enhancing luminescence from near surface silicon has been further confirmed by other authors [45, 46]. The main problem of this approach for a silicon laser is that it does not remove the two main problems of silicon which prevent population inversion, i.e. Auger recombination and free-carrier absorption [44].

Finally, a problem is also related to the wavelength of emission of these bulk silicon LEDs which is resonant with the silicon bandgap: that means that it is very difficult to control the region where the light is channelled in silicon if one wants to use these LEDs as a source for optical interconnects. Light will propagate through the wafer and will be absorbed in unwanted places.

3.2. Silicon nanocrystals

Another way to increase the emission efficiency of silicon is to turn it into a low dimensional material and, hence, to exploit quantum confinement effects to increase the radiative probability of carriers. This approach has been pioneered by the work on porous silicon (PS) [49] which shows that when silicon is partially etched in an HF solution via an electrochemical attack, the surviving structure is formed by small nanocrystals or nanowires which show bright red luminescence at room temperature. The explanation of the observed high luminescence efficiency in PS was

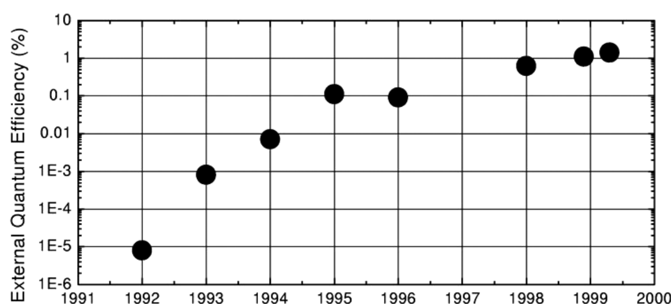

Figure 15. External quantum efficiency of PS LEDs over the year. The record in efficiency to date is that of [51].

(i) quantum confinement which leads to an enlargement of the bandgap and to an increased recombination probability,
(ii) the spatial confinement of the free carriers which prevents them reaching non radiative recombination centres and
(iii) the reduction of the refractive index of the material which increases the extraction efficiency via refractive index matching.

This result has motivated many research efforts in order to exploit these properties in LEDs [50]. The evolution of PS LED performances over the year is reported in figure 15 [51].

The PS approach has however a draw-back in the high reactivity of the spongelike texture which causes the rapid ageing of the LED and an uncontrollable variation of the LED performance with time [50]. No optical gain was reported in bulk PS. From PS, silicon nanocrystals (Si-nc) can be obtained by scrapping or ultrasonically dispersing PS [52]. Then the surface chemistry can be adjusted and, in particular, oxide passivated. Evidence of amplification in these materials has been presented [53].

An alternative way is to produce silicon nanocrystals (Si-nc) in a silica matrix to exploit the quality and stability of the SiO_2/Si interface and the improved emission properties of low dimensional silicon. Many different approaches have been proposed to form the silicon nanocrystals [13, 53]. The most widely used are based on the deposition of sub-stoichiometric silica films, with a large excess of silicon, followed by a high temperature annealing [54]. The annealing causes a phase separation between the two constituent phases, i.e. silicon and SiO_2 with the formation of small silicon nanocrystals. The size and density of the Si-nc can be controlled by the deposition and the annealing parameters. Recently, the anneal of amorphous SiO/SiO_2 superlattices has been proposed to control the size distribution. Almost monodispersed size distribution has been demonstrated [55].

The luminescence properties of Si-nc are very similar to those of PS: a wide emission band is observed at room temperature whose spectral position depends on the Si-nc sizes. In these systems optical gain has been observed [37, 53, 56–62]. Optical gain in Si-nc has been revealed as a superlinear increase of the luminescence intensity as a function of the pumping rate [53, 59], as the measurements of amplified spontaneous emission (ASE) in a waveguide geometry [37, 56, 57, 60–62] (see figures 16–18), as probe amplification in transmission experiments under high pumping excitation [37] or as collimated and speckled patterned emissions which show the coherent properties of the emitted light [59]. Some concerns have been raised about the methods used to measure the gain [63]. Almost all the authors agree on the fact that the gain is due to localized state recombinations either in the form of silicon dimers or in the form of Si=O bonds formed at the interface between the Si-nc and the oxide

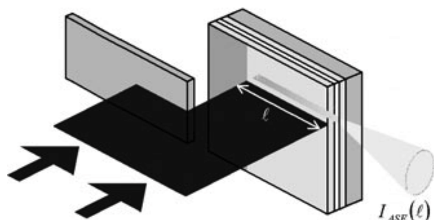

Figure 16. Sketch of the variable stripe length method to measure optical gain. The amplified spontaneous luminescence intensity I_{ASE} is collected from the edge of the sample as a function of the excitation length *l*. The laser beam is focused on a thin stripe by a cylindrical lens.

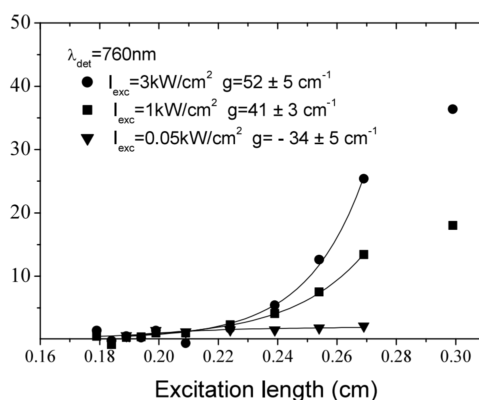

Figure 17. Room temperature VSL curves on a Si-nc sample as a function of the pumping intensities. The detection wavelength was 760 nm. By increasing the pumping intensity from 0.05 kW cm^{-2} to 1 kW cm^{-2} the optical losses turn into optical gain. The values of optical gain become saturated at an intensity of 3 kW cm^{-2} (from [62]).

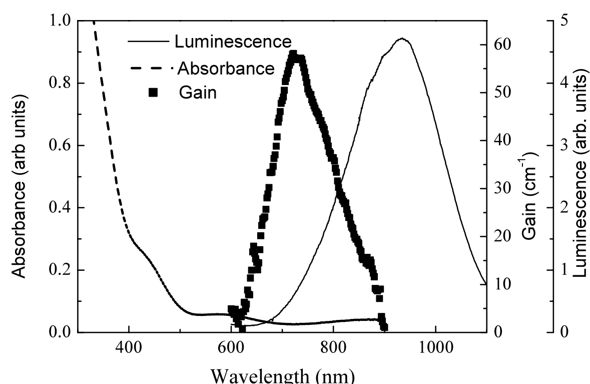

Figure 18. Absorbance (dashed curve), modal gain spectrum (solid squares) and luminescence spectrum (solid curve) for a Si-nc sample (from [62]).

or within the oxide matrix. The suggested scheme to explain population inversion, and hence gain, is a four-level model where a large lattice relaxation of the photoexcited localized centre gives rise to the four levels (figure 19) [56, 62].

Very interesting information can be achieved by time resolved experiments of the ASE from Si-nc in a waveguide geometry [56, 57, 62]. Figure 20 reports the decay lineshape of the ASE both as a function of the pumping fluences (figure 20(a)) and as a function of the excited length (figure 20(b)). In addition to the usual slow recombination of Si-nc (microseconds range), a fast contribution (nanosecond timescale) is observed which grows up either by increasing the fluence or by increasing the excitation length. This last observation rules out Auger recombination as the cause of the fast component because of its strongly non-linear dependence on the photo-excited carrier concentration, which in figure 20(b) is constant for all the various lengths. The origin of the fast component in these Si-nc is stimulated emission. This is also supported by other experimental data.

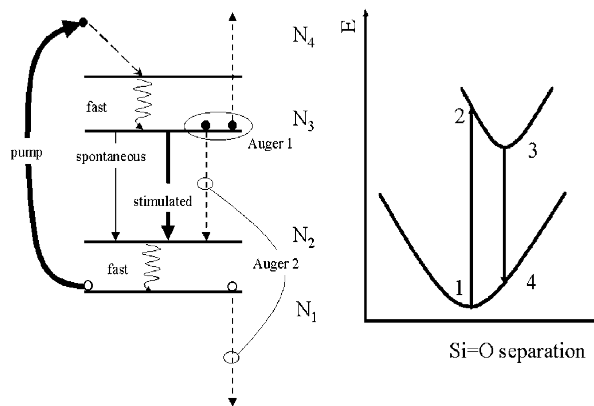

Figure 19. Left, effective four-level system based on the results of figure 18, which has been introduced to model qualitatively the recombination dynamics under gain conditions. From level 3 the excited carriers can recombine by spontaneous, stimulated or Auger recombinations. Right, schematic diagram of the energy configuration diagram of the silicon nanocrystals in an oxygen rich matrix. Localized radiative states are formed inside the nanocrystal bandgap by the interface oxygen atoms. The excited nanocrystal state can occur at a different lattice coordinate with respect to the ground state (from [62]).

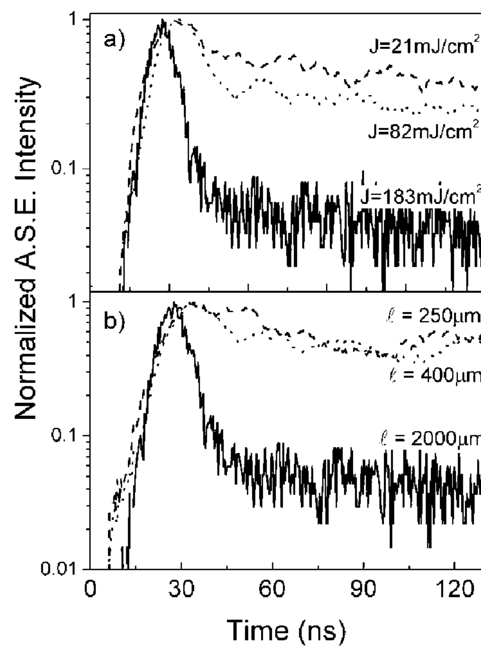

Figure 20. (a) Normalized ASE measured under VSL geometry with a pumping length $l = 2$ mm at the different pumping fluences reported in the figure. The measured sample is a Si-nc waveguide. Excitation wavelength was 355 nm. (b) Here the effect of the pumping length l on the fast ASE dynamics is shown. The pumping fluence is fixed at 183 mJ cm^{-2} and only the pumping length is varied according to the values reported in the figure (from [62]).

Figure 21(a) reports the exponential increase of the fast component intensity as a function of the photoexcited volume (which yields a net modal gain of 12 cm^{-1} under these pumping conditions). Figure 21(b) shows a clear fluence threshold over which the ASE increases

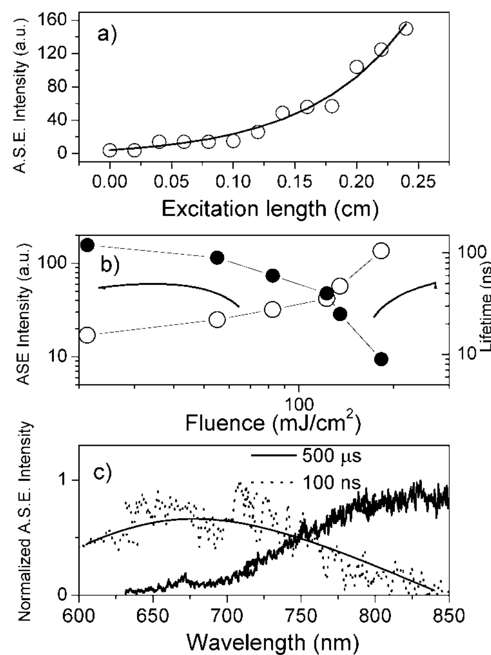

Figure 21. (a) Points: ASE peak intensity at 760 nm versus the excitation length at a pump fluence of 200 mJ cm^{-2}. Full curve: fit of the experimental data with the one-dimensional amplifier model which yields a net modal gain value of 12 ± 3 cm^{-1}. (b) Open circles: ASE peak intensity of the fast component versus the pumping fluence. Black discs: $1/e$ lifetime of the ASE decay as a function of the pumping fluence. Excitation length was approximately $l = 2$ mm. (c) ASE spectra measured for a fixed excitation length $l = 2$ mm and pumping fluence of 200 mJ cm^{-2} for two different integration time windows: dotted curve, 100 ns after the excitation; full curve, 500 μs after the excitation. All the data in this figure have been taken with an excitation wavelength of 355 nm (from [62]).

superlinearly with the fluences, and the decay lifetime of the emission decreases to a few nanoseconds. Figure 21(c) shows that the spectral shape of the fast component is different from the one of the slow component reflecting the typical blue shift of the gain band with respect to the luminescence (figure 18) which supports the four-level model of figure 19. The four-level model is also able to reproduce the decay of the luminescence at high fluences for Si-nc as demonstrated in figure 22. In the simulation of figure 22 both stimulated emission and Auger recombination are taken into account. At the peak fluence the lifetimes associated with these two processes are only slightly different. It is also this delicate interplay between Auger recombination and stimulated emission that governs the optical gain in Si-nc. As discussed in [62], the Si-nc density should be large enough to yield a significant optical gain. This means that optical gain cannot be achieved in all Si-nc samples. It is interesting to note that the data of figure 22 cannot be fitted with only Auger recombinations, even with peak Auger lifetimes as short as 90 ps. The contribution from stimulated emission is needed to accurately reproduce the luminescence decay.

The Si-nc system is very promising to achieve a laser. Indeed, other key ingredients for a laser have been demonstrated. Vertical optical micro-cavities based on a Fabry–Perot structure with mirrors constituted by distributed Bragg reflectors (DBRs) and where the central layer is formed by Si-nc dispersed in SiO_2 have been already fabricated [64]. The presence of the thick SiO_2 layer needed to form the DBR can be a problem for electrical injection when

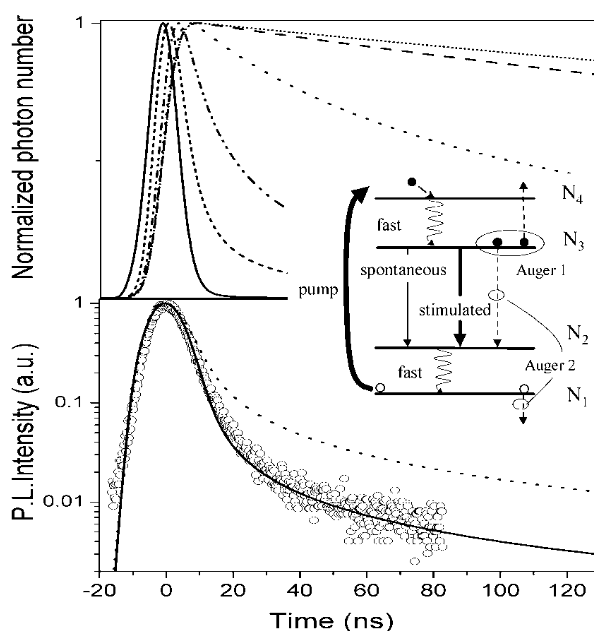

Figure 22. Top panel, simulations of the normalized PL intensity as a function of the incident photon flux ϕ_P. The peak of the incident photon flux ϕ_P was varied between 10^{16} and 10^{24} photons s^{-1} cm^{-2}. The main parameters used in the simulation were the pump absorption cross-section $\sigma_P = 10^{-14}$ cm^2, the emission cross-section $\sigma = 10^{-17}$ cm^2, the active centre concentration $N = 8 \times 10^{18}$ cm^{-3}, the spontaneous emission factor $\beta = 4.5 \times 10^{-4}$ and the optical losses $\alpha = 25$ cm^{-1}. No Auger recombination has been considered here. Bottom panel, PL decay (○) of Si-nc produced by PECVD deposition of 46 at.% Si annealed at 1250 °C for 1 h. The solid line is a simulation obtained with the same parameters as in the top panel plus an effective Auger coefficient $C_A = 10 \times 10^{-10}$ cm^{-3} s^{-1} (peak Auger lifetime of 3 ns) and a pump photon flux of 5×10^{22} photons s^{-1} cm^{-2}. The dashed line is a simulation where no stimulated emission was present, only Auger recombination. In this case an Auger coefficient of $C_A = 2 \times 10^{-8}$ cm^{-3} s^{-1} (peak Auger lifetime of 90 ps) is needed (courtesy of L Dal Negro).

current has to flow through the DBR. Lateral injection schemes can avoid these problems. On the other hand, the electrical injection into the Si-nc is a delicate task by itself[1]. Bipolar injection is extremely difficult to achieve. Despite some claims, most of the reported Si-nc LEDs are impact ionization devices: electron–hole pairs are generated by impact ionization by the energetic free carriers injected through the electrode. By exploiting impact ionization Si-nc LEDs have been demonstrated with EL spectra overlapping luminescence spectra, onset voltage as low as 5 V and efficiencies in excess of 0.1% [66]. Some unconfirmed claims of near-laser action of Si-nc LEDs have appeared in the literature [67, 68].

The problem of gain in Si-nc still has some unanswered issues:

(i) what is the role played by the Si-nc and by the embedding medium?
(ii) what are the key parameters which determine the presence of gain in the Si-nc?
(iii) is the nanocrystal interaction influencing the gain?
(iv) are low-losses active waveguides possible to achieve?
(v) what is the precise nature of the four levels in the model, in particular the location and role of Si–O bonds?

[1] An introduction and up-to-date review can be found in [65].

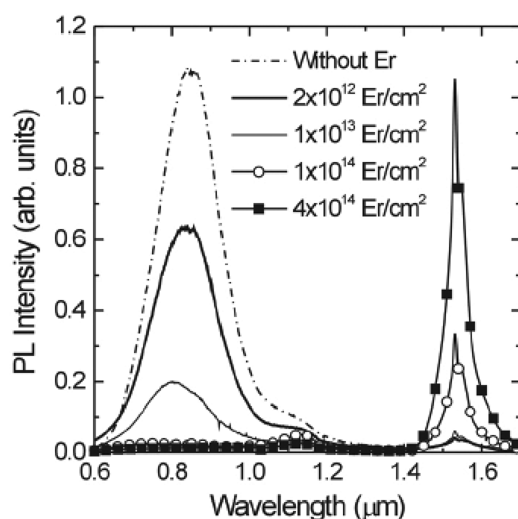

Figure 23. Room temperature PL spectra of Er implanted Si nanocrystals at different Er doses. The pump power of the laser beam was 50 mW (after [74]).

3.3. Er coupled silicon nanocrystals

The recent increase in the transmission capacity of optical fibre based communication is also related to the availability of all-optical amplifiers based on Er doped fibres [69]. In this amplifier, a silica optical fibre is doped with Er^{3+} ions, whose internal atomic-like transition at 1.54 μm is exploited to achieve light amplification. In the past, several attempts have been made to reproduce a similar materials system in silicon. Several breakthroughs have been recently achieved in the field of Er doping of crystalline Si that allowed fabrication of LEDs operating at room temperature [71–73].

What it is more interesting for light amplification studies is the experimental finding of a strong enhancement of the Er luminescence when Er is implanted or deposited in a SiO_2 matrix where Si-nc have been formed, i.e. Si-nc act as sensitizers for erbium ions [74, 75]. Non-radiative de-excitation processes are reduced by widening the Si bandgap and thus avoiding one of the most detrimental sources of Er luminescence quenching. Indeed, the thermally activated back-transfer of excitation from Er^{3+} to Si-nc becomes less efficient than in bulk Si since the energy mismatch for the process becomes larger. Widening of the bandgap also produces a reduction in the free-carrier concentration, thus limiting the Auger processes. As demonstrated in figure 23, a strong luminescence comes from Er ions that are pumped through an electron–hole mediated process in which photo-excited excitons from Si nanocrystals transfer their energy to Er ions [74]. The number of Si-nc coupled to a single Er ion is still a debated issue (between one and ten) [74, 76]. As concerns where Er is placed, from high resolution luminescence it is clear that most of the Er is in the SiO_2 matrix, which is an ideal situation if one looks at reproducing the environment which is found in an Er doped fibre amplifier. Hence, Er coupled Si-nc benefits from the advantages of both silicon (efficient excitation) and SiO_2 (weak non-radiative processes, i.e. negligible temperature quenching of the luminescence), while it avoids their disadvantages (low excitation efficiency in SiO_2 and strong non-radiative processes in bulk Si). Indeed, MOS light emitting devices operating at room T have been made with this system, where a quantum efficiency larger than 1% [38] is demonstrated. Even higher efficiencies (10%) are reported for Er in silicon rich oxide films; however, in this system reliability is still an issue [39].

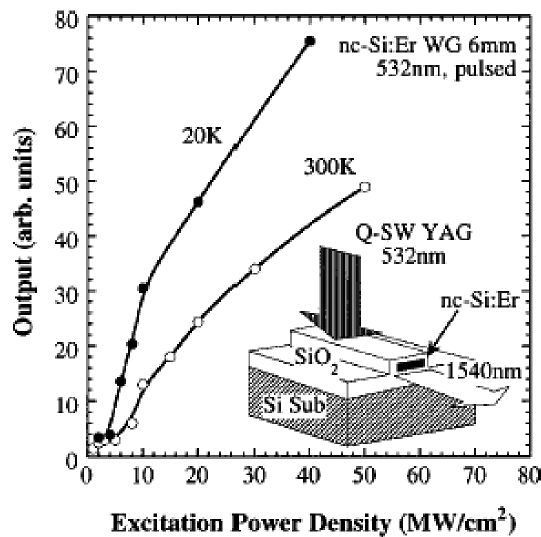

Figure 24. Pumping power density dependence of the 1540 nm emission of a 6 mm Er doped nc-Si waveguide (after [77]).

The layer co-doped with Si-nc and Er^{3+} ions has a refractive index which is larger than that of SiO_2, i.e. waveguides can be formed with a core containing Er^{3+} coupled to Si-nc. Experiments have shown luminescence increases (figure 24) [77] or even evidence of signal enhancement (figure 25) [78] are present in these waveguides. Even though no net optical gain was measured, an enhancement in the probe transmission at 1.535 μm was observed as the pump power was increased. By rather crude approximations, it is possible to write that the probe transmission when the pump is on, $I(P)$, is related to the probe transmission when the pump is off, $I(0)$, by SE $\equiv I(P)/I(0) = \exp(2(\sigma N_2 \Gamma)L)$, where SE is the signal probe enhancement, σ is the Er^{3+} emission cross-section at 1.535 μm, N_2 the density of excited Er ions, Γ the optical mode confinement factor and L the waveguide length. A fit to the experimental data yields an increased Er^{3+} emission cross-section with respect to Er ions in silica or in silicon (table 1) [40]. This is a quite unexpected result, which has however been confirmed by other research groups. The reason is still unclear; one can speculate about the role of the dielectric environment which is modified by the presence of the Si-nc [76]. What makes this finding interesting is the possibility of significantly reducing the cavity length in an amplifier or laser below the one usually employed in the silica doped fibre systems. Sizeable gain can be further obtained by low Er doping concentrations. To summarize the very interesting properties of the Er^{3+} coupled Si-nc system, table 1 compares the main cross-sections of Er^{3+} in silica and silicon and coupled with Si-nc.

The system Er^{3+} coupled to Si-nc is very promising for laser applications because the active material (Er^{3+} in SiO_2) has already shown lasing properties. In addition, the technology to produce the material is very compatible with CMOS processing. Microcavities with excellent luminescence properties have been also demonstrated [64], which allows design of both edge emitting and vertical emitting laser structures. The issue related to electrical pumping of the active material, which was believed to be a major short-cut of this approach, can be solved as extremely high efficiency LEDs have been demonstrated [38, 39]. A still open issue is to engineer the waveguide losses in order to be able to measure net optical gain and not only signal enhancement in a pump and probe experiment. This seems only a problem of time and

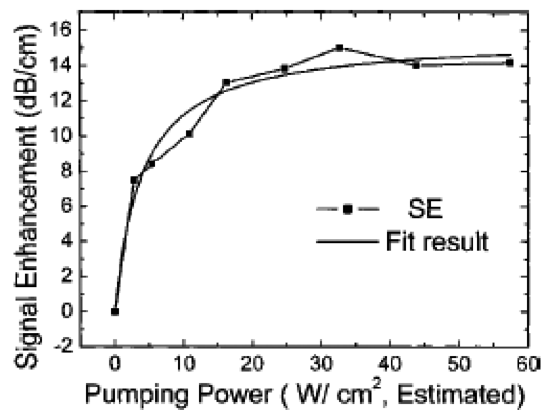

Figure 25. Pump power dependence of the signal enhancement SE and of a theoretical fit. An SE of up to 14 dB cm^{-1}, implying a possible net gain of up to 7 dB cm^{-1}, is found. From the fit, an emission cross-section of 2×10^{-19} cm^2 and an effective excitation cross-section of $>10^{-17}$ cm^2 at 477 nm was deduced (from [78]).

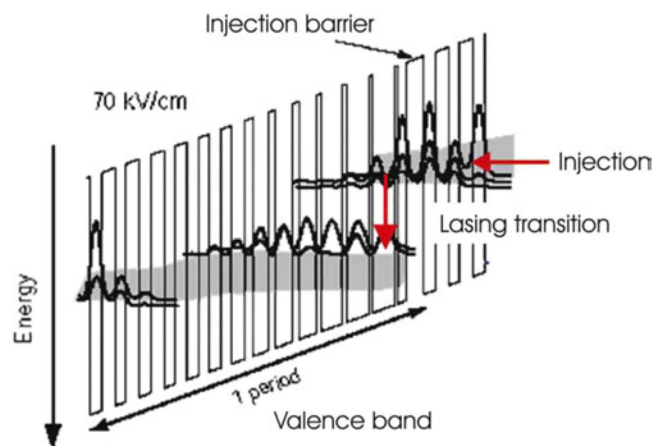

Figure 26. Schematic valence band diagram of one stage of the structure, under an applied electric field of 70 kV cm^{-1}. Only the HH band and the modulus squared of the relevant HH wavefunctions are shown for clarity. Note that the axis of the energy is turned upside down. Each period, starting from the injection barrier, consists of the following sequence of Si barrier (roman) and $Si_{0.2}Ge_{0.8}$ (bold) in Å: 25/**11**/4/**26**/5/**26**/6/**24**/7/**21**/8/**19**/9/**18**/10/**17**/11/**15**/12/**15**/13/**14**/15/**14**/16/**13**/17/**13**. The underlined numbers correspond to doped layers with a boron concentration of 5×10^{17} cm^{-3} (from [88]).

research efforts. Then further work should be spent to optimize the gain with respect to the waveguide parameters and develop a suitable optical cavity which can be electrically injected.

3.4. Si/Ge quantum cascade structures

One route to avoid the fundamental limitation to lasing in silicon, i.e. its indirect bandgap, is to avoid using interband transitions. Indeed, if one exploits only intraband transition, e.g. intra-valence-band transition, no fundamental problems exist to impede lasing in silicon [82]. This

Table 1. Summary of the various cross-sections related to Er^{3+} in various materials.

	Er in SiO_2 (cm^2)	Er in Si (cm^2)	Er in Si-nc (cm^2)	Reference for Er in Si-nc
Effective excitation cross-section of luminescence at a pumping energy of 488 nm	$(1–8) \times 10^{-21}$	3×10^{-15}	$(1.1–0.7) \times 10^{-16}$	[79, 80]
Effective excitation cross-section of EL		4×10^{-14}	1×10^{-14} by impact ionization	[38]
Emission cross-section at 1.535 μm	6×10^{-21}		2×10^{-19}	[40]
Absorption cross-section at 1.535 μm	4×10^{-21}	2×10^{-20}	8×10^{-20}	[81]

is indeed the approach of the quantum cascade (QC) Si/Ge system. With SiGe QC lasers, one is trying to use the concept that has already been successful in III–V semiconductors, which is advancing as a viable option for mid-IR emission, covering today a large wavelength range, 3–24 μm [83].

The idea of the device is shown in figure 26. The QC scheme can be implemented in the conduction or valence band. However, to achieve a conduction band discontinuity the growth of a Si/Ge superlattice on a relaxed SiGe buffer is necessary. For pseudomorphic growth on a Si substrate most of the band offset occurs in the valence band. Hence, the cascading scheme is usually designed in the valence band [84]. This differs from QC lasers based on III–V semiconductors that employ electron cascade structures. In figure 26, the valence band diagram of a cascading stage of a hole-injected p–i–p valence band device is shown. Injected holes make a vertical transition between subbands, and then they cascade down the electrically biased staircase. In order to assist population inversion, the lower laser level is rapidly depopulated by relaxation within the miniband. Practically, one has two identical active regions connected by an injector. EL from a SiGe QC structure grown on Si has recently been demonstrated [84, 88].

Starting from the possibility of monolithic integration with silicon microelectronics, the Si/SiGe system is more interesting than III–V heterostructures for QC laser applications. The non-polar electron–phonon interaction is the dominant loss process in III–V QC lasers. In silicon, due to the covalent bonding, the non-polar phonon scattering is absent. The optical phonon energy in Si is much higher than in GaAs (64 meV compared with 36 meV), providing a larger frequency window within which (non-polar) optical phonon scattering is suppressed. In Si the thermal conductivity is much larger than that of GaAs, giving better prospects of CW operation at non-cryogenic temperatures. On the other hand, some constraints are present [85]: the necessity to work in the valence band and thus the higher effective masses of the charge carriers, limited band offset of approximately 80 meV per 10% Ge concentration and splitting into heavy hole (HH) and light hole (LH) bands. Moreover, the high amount of strain, due to the lattice mismatch between Si and Ge, sets an upper limit to the number of wells per cascade and the number of cascades, as well as the thickness and Ge content of each individual well. Due to the mentioned constraints, the developed Si/SiGe cascade structure is a drastically simplified version of the typical III–V QC structures. As shown in figure 26, in a practical QC structure each cascade consists of only a few wells [85].

Figures 27 and 28 show the typical EL spectra recorded in QC structures grown on Si substrates [87, 88]. The levels involved are valence levels; the radiative transition is between HH states. The quantum efficiency estimate is about 10^{-5} for EL [85–88]. Temperature-

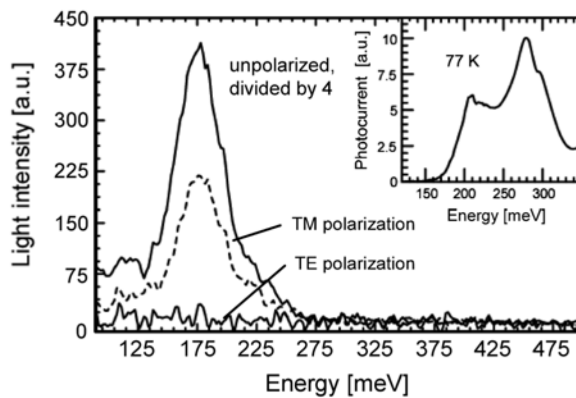

Figure 27. EL spectra of the sample with 15 repetitions, taken at 80 K with and without a polarizer placed in the light path. The parameters are 4.7 V, 550 mA, 94 kHz and a duty cycle of 10%. The polarized EL is measured at 5.2 V, 650 mA and a 20% duty cycle. The inset shows the results of a photocurrent measurement at 77 K (from [88]).

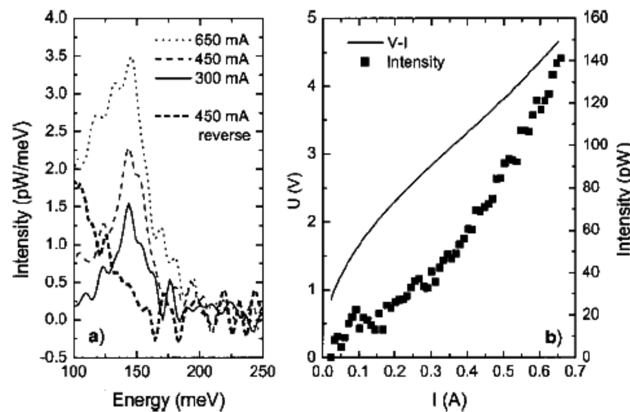

Figure 28. (a) Current-dependent EL spectra in forward bias and spectrum at reverse bias at 80 K. (b) I–V curve and integrated EL intensity (from [87]).

dependent measurements show nearly identical spectra between 20 and 90 K and a broadening and vanishing of the peak at about 160 K. It is possible to improve these results controlling the large accumulation of strain imposed by the use of a Si substrate. This has been done by using a $Si_{0.5}Ge_{0.5}$ substrate and growing on it strain compensated $Si_{0.2}Ge_{0.6}$/Si quantum wells. Intersubband transitions have been observed by absorption measurements at 235, 262 and 325 meV changing the well width from 3.5 to 2.5 nm; peaks are observed up to room temperature [88]. For similar structures EL has been detected at 80 K [88].

The QC concept works for III–V semiconductors. The SiGe system has some advantages and a fundamental limit posed on the number of periods of successive QW cascades which is given by the critical thickness for the formation of misfit dislocation. Hence, even though these devices show interesting EL properties for the prospect of the development of a Si based laser, highly evolved cascade structures have to be realized. As the gain per single element is low due to the nature of the intraband transition, a large number of cascading structures will be needed to accumulate a macroscopic gain. In fact, no stimulated emission in SiGe

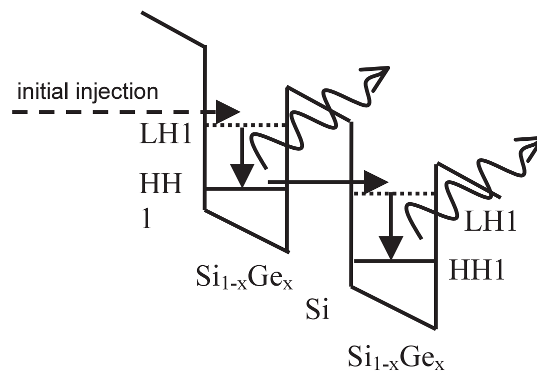

Figure 29. Schematic valence band profile of a Si/SiGe quantum staircase laser operating via radiative LH1–HH1 transitions (from [92] with kind permission of Kluwer Academic Publishers).

QC structures has been reported to date. In addition, all these have to be integrated within a waveguide cavity. In addition, the emission wavelength is different from those commonly used for optical interconnects. A waveguide for these wavelengths can be realized by using SOI substrates or thick, relaxed SiGe graded buffer. The other photonic components have still to be developed to achieve a photonic integrated system. Although some authors propose to use a QC laser for free-air optical interconnects, such a Si/Ge QC laser will be of little use for silicon photonics if all other compatible elements will not be developed.

3.5. THz emission

A gap in the frequency spectrum of electromagnetic waves opens across the THz region, where no semiconductor sources are available. At low frequencies, sources are made by electronic oscillators (high speed transistors) while at high frequencies the sources are made by injection lasers. Recently, a THz laser has been demonstrated by using III–V semiconductors which shows the way to cover this THz gap [89]. With the same aim, and using the many advantages of the SiGe system over the III–V systems for these frequencies, a research effort is made to implement the QC concept and make a laser in these frequency regions [90–92]. A typical structure is shown in figure 29 which by using p-type heterostructures is designed to emit radiation from LH–HH transitions. In this way both edge emission and surface-normal THz emission might be obtained. Growth of p-Si/SiGe QC structures comprising up to 100 periods has been demonstrated using low pressure CVD via a strain balanced approach on virtual substrates. Intersubband THz EL from a range of Si/SiGe QC structures has been observed in both edge and surface-emission geometries. An example is shown in figure 30. The LH–HH intersubband lifetime was measured to be ∼20 ps, which is over an order of magnitude longer than high temperature values in III–V heterostructures, implying that a Si/SiGe THz QC laser may be capable of much higher operating temperatures than corresponding III–V devices. Emission power levels comparable to the one reported on III–V devices before laser processing have been measured which indicate that there are good prospects for realization of a THz Si/SiGe QCL via further optimization of the active region and appropriate cavity design [92].

Another approach to THz laser emission in silicon has been developed [93–96]. The idea is to make a THz laser using intra-shallow donor optical transitions in silicon. A band diagram showing the lasing transition is reported in figure 31. Very narrow spectral emission and the

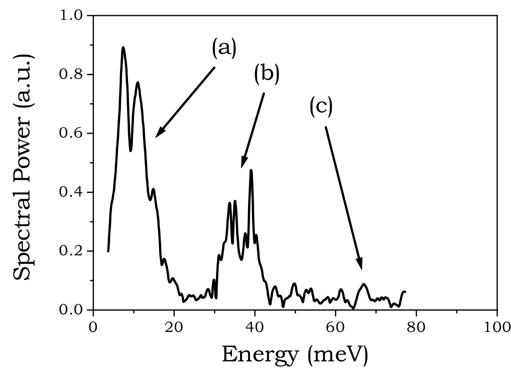

Figure 30. FTIR edge-emission spectrum for a QC structure, at a temperature of 4.2 K. The pulsed bias voltage was 7 V with a 10% duty cycle. The features marked (a), (b) and (c) correspond to the theoretically calculated emission peaks for the LH1–HH1, HH2–HH1 and LH2–HH1 intersubband transitions, respectively (from [92] with kind permission of Kluwer Academic Publishers).

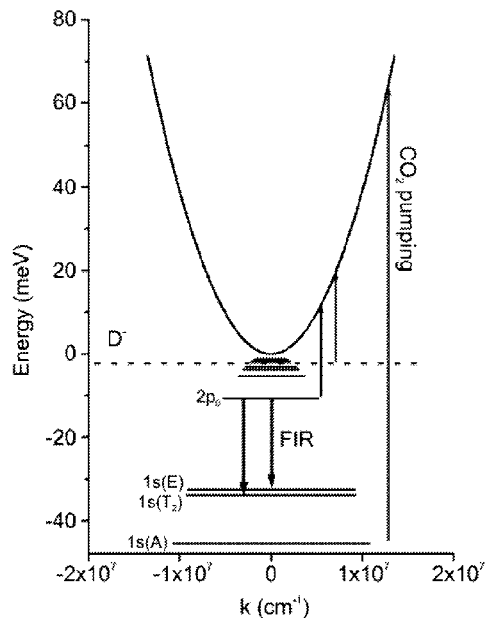

Figure 31. Optical transitions in Si:P. The dashed line represents the energy level of the D^- centre state (from [96]).

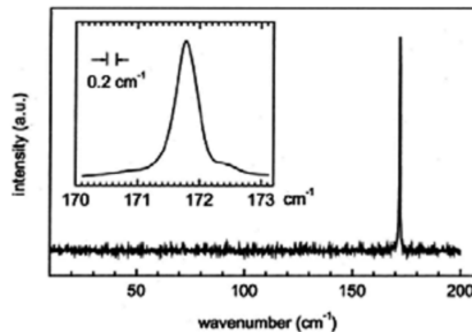

Figure 32. Stimulated emission spectrum from Si:Sb. The emission curve is identified with the $2p_0 \rightarrow 1s$ intracentre Sb transition (from [96]).

light intensity threshold versus pumping power are reported in figures 32 and 33. All these data should indicate that lasing has been achieved in this system. However, some points need to be clarified, such as the optical mode pattern in the simple cavity structure used, the evolution from spontaneous to stimulated emission and the coherent property of the light. Other concerns are related to the dilute doping of the system in order to avoid impurity–impurity interaction which will prevent population inversion and the schemes for electrical injection. It is clear that the use of THz laser sources for silicon microphotonics requires a complete reshaping of the scheme developed up to now.

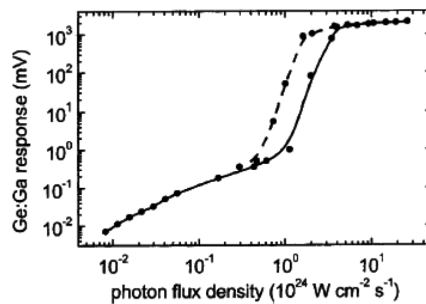

Figure 33. Dependence of the emission on the pump power for 9.6 μm excitation (dashed curve) or the 10.6 μm excitation (solid curve) (from [96]).

4. Conclusion

Throughout this review, I have tried to describe the status of silicon microphotonics and the recent advances that cause people to be optimistic to the realization of an active silicon light source. Indeed, many claims to have a silicon based laser within a short period have appeared in the literature by many of the researchers involved in this field [97]. If this objective is realized all the major building blocks for monolithic silicon microphotonics will be available.

The final vision is to have Si microphotonics participating in every global application of the photonics industry: communications, computing, information displays, optical-and-infrared imaging, medicine, optical printing, optical command-and-control, optical sensing of physical chemical and biological inputs, optical signal processing, optical storage and optical control of microwave devices or systems [98]. We indeed propose silicon as the unifying material where the next generation of photonics devices will be realized.

Acknowledgments

It is a pleasure to acknowledge all my co-workers in the Silicon Photonics group of Trento (http://science.unitn.it/~semicon/) and the financial support of the EC through the MELARI cluster and the Sinergia project, of MIUR through the PRIN2000 and PRIN2002 projects, of INFM through the Luna, Ramses, SMOG and RANDS projects and of Provincia Autonoma di Trento through the Profill project. L C Andreani, P Bellutti, U Gösele, F Iacona, L C Kimerling, A Lui, S Ossicini, F Priolo, D Wiersma are also thanked for valuable discussions and collaboration on this topic.

References

[1] Plummer J D, Deal M D and Griffin P B 2000 *Silicon VLSI Technology* (Upper Saddle River, NJ: Prentice-Hall)
[2] Clemens J T 1997 *Bell Lab. Tech. J.* **Autumn** 76
[3] International Technology Roadmap for Semiconductors, 2000 Update, Interconnect (http://public.itrs.net.)
[4] Risch L 2002 *Mater. Sci. Eng.* C **19** 363
[5] Theis T N 2000 *IBM J. Res. Dev.* **44** 379
[6] ftp://download.intel.com/labs/eml/download/EML_opportunity.pdf
[7] Miller D A 2000 *Proc. IEEE* **88** 728
[8] Moore S K 2002 *Spectrum IEEE*
[9] http://mph-roadmap.mit.edu/TWiGs.html#Si
[10] http://www.intel.com/research/silicon/index.htm
http://www.zurich.ibm.com/st/optics/index.html

http://us.st.com/stonline/bin/hilite.exe?file=/stonline/press/magazine/challeng/3rdedi02/chal4.htm&words=PHOTONIC
[11] Kimerling L C 2000 *Appl. Surf. Sci.* **159/160** 8
[12] Soref R A 1993 *Proc. IEEE* **81** 1687
[13] Bisi O, Campisano S U, Pavesi L and Priolo F (ed) 1999 *Silicon Based Microphotonics: from Basics to Applications* (Amsterdam: IOS Press)
[14] Masini G, Colace L and Assanto G 2002 *Mater. Sci. Eng.* B **89** 2–9
[15] Pal B P 1993 *Progress in Optics* vol 32, ed E Wolf (Amsterdam: Elsevier) p 1
[16] Miya T 2000 *IEEE J. Sel. Top. Quantum Electron.* **6** 38
[17] Bulla D A P *et al* 1999 *IMOC'99 Proc. IEEE* p 454
[18] Hilleringmann U and Goser K 1995 *IEEE Trans. Electron. Devices* **42** 841
[19] Cocorullo G, Della Corte F G, Iodice M, Rendina I and Sarro P M 1998 *IEEE J. Sel. Top. Quantum Electron.* **4** 983
[20] Lee K K, Lim D R, Luan Hsin-Chiao, Agarwal A, Foresi J and Kimerling L C 2000 *Appl. Phys. Lett.* **77** 1617
[21] Rosa M A, Ngo N Q, Sweatman D, Dimitrijev S and Harrison H B 1999 *IEEE J. Sel. Top. Quantum Electron.* **5** 1249
[22] Ang T W, Reed G T, Vonsovici A, Evans A G R, Routley P R and Josey M R 1999 *Electron. Lett.* **35** 977
[23] Jalali B, Yegnanarayanan S, Yoon T, Yoshimoto T, Rendina I and Coppinger F 1998 *IEEE J. Sel. Top. Quantum Electron.* **4** 938
[24] Bestwick T 1998 *48th IEEE Conf. on Electronic Components and Technology (May 1998)* pp 566–71
[25] Zimmermann H 2000 *Integrated Silicon Optoelectronics* (New York: Springer)
[26] Csutak S M, Schaub J D, Wu W E, Shimer R and Campbell J C 2002 *J. Lightwave Technol.* **20** 1724
[27] Yang M, Rim K, Rogers D L, Schaub J D, Wleser J J, Kuchta D M, Boyd D C, Rodier F, Rabidoux P A, Marsh J T, Icknor A D, Yang Q, Upham A and Ramac S C 2002 *IEEE Electron. Device. Lett.* **23** 395
[28] Masini G, Colace L, Assanto G, Wada K and Kimerling L C 1999 *Electron. Lett.* **35** 1467
Colace L, Masini G, Assanto G, Luan H C, Wada K and Kimerling L C 2000 *Appl. Phys. Lett.* **76** 1231
[29] Winnerl S, Buca D, Lenk S, Buchal Ch, Mantl S and Xu D X 2002 *Mater. Sci. Eng.* B **89** 73
[30] El kuedi M *et al* 2002 *J. Appl. Phys.* **92** 1858
[31] Coppola G, Irace A, Breglio G, Iodice M, Zeni L, Cutulo A and Sarro P M 2003 *Opt. Laser Eng.* **39** 317
[32] Kato K and Tohmori Y 2000 *IEEE J. Sel. Top. Quantum Electron.* **6** 4
[33] Kimerling L 2003 *Towards the First Silicon Laser (NATO Series vol 93)* ed L Pavesi, S Gaponenko and L Dal Negro (New York: Kluwer) p 465
[34] Chen R T *et al* 2000 *Proc. IEEE* **88** 780
[35] at press Ossicini S, Pavesi L and Priolo F 2003 *Light Emitting Silicon for Microphotonics (Springer Tracts in Modern Physics)* (Berlin: Springer)
[36] Green M A, Zhao J, Wang A, Reece P J and Gal M 2001 *Nature* **412** 805
[37] Pavesi L, Dal Negro L, Mazzoleni C, Franzò G and Priolo F 2000 *Nature* **408** 440
[38] Iacona F, Pacifici D, Irrera A, Miritello M, Franzó G, Priolo F, Sanfilippo D, Di Stefano G and Fallica P G 2002 *Appl. Phys. Lett.* **81** 3242
[39] Castagna M E, Coffa S, Caristia L, Messina A and Bongiorno C 2002 *Proc. ESSDDERC2002* p 439
[40] Han Hak-Seung, Seo Se-Young, Shin Jung H and Park Namkyoo 2002 *Appl. Phys. Lett.* **81** 3720
[41] Pavesi L, Gaponenko S and Dal Negro L (ed) 2003 *Towards the First Silicon Laser (NATO Series vol 93)* (New York: Kluwer)
[42] Ng W L, Lourenço M A, Gwilliam R M, Ledain S, Shao G and Homewood K P 2001 *Nature* **410** 192
[43] Zhao J, Green M A and Wang A 2002 *J. Appl. Phys.* **92** 2977
[44] Dumke W P 1962 *Phys. Rev.* **127** 1559
[45] Gusev O B, Bresler M S, Yassievich I N and Zakharchenya B P 2003 *Towards the First Silicon Laser (NATO Series vol 93)* ed L Pavesi, S Gaponenko and L Dal Negro (New York: Kluwer) p 21
[46] Sotta D 2002 Milieux emetteurs de lumiere et microcavites optique en silicium monocristallin sur isolant *Thesis* Specialite physique, Universite Joseph Fourier Grenoble I
[47] Delerue C, Lannoo M, Allan G, Martin E, Mihalcescu I, Vial J C, Romestain R, Muller F and Bsiesy A 1995 *Phys. Rev. Lett.* **75** 2229
[48] Jonsson P, Bleichner H, Isberg M and Nordlander E 1997 *J. Appl. Phys.* **81** 2256
[49] Canham L T 1990 *Appl. Phys. Lett.* **57** 1046
[50] Bisi O, Ossicini S and Pavesi L 2000 *Surf. Sci. Rep.* **264** 1–126
[51] Gelloz B and Koshida N 2000 *J. Appl. Phys.* **88** 4319
[52] Yamani Z, Thompson H, AbuHassan L and Nayfeh M H 1997 *Appl. Phys. Lett.* **70** 3404

[53] Nayfeh M H, Barry N, Therrien J, Akcakir O, Gratton E and Belomoin G 2001 *Appl. Phys. Lett.* **78** 1131
[54] Iacona F, Franzò G and Spinella C 2000 *J. Appl. Phys.* **87** 1295
[55] Zacharias M, Heitmann J, Scholz R, Kahler U, Schmidt M and Bläsing J 2002 *Appl. Phys. Lett.* **80** 661
[56] Dal Negro L, Cazzanelli M, Daldosso N, Gaburro Z, Pavesi L, Priolo F, Pacifici D, Franzò G and Icona F 2003 *Physica* E **16** 297
[57] Khriachtchev L, Rasanen M, Novikov S and Sinkkonen J 2001 *Appl. Phys. Lett.* **79** 1249
[58] Nayfeh M H, Rao S and Barry N 2002 *Appl. Phys. Lett.* **80** 121
[59] Luterova K, Pelant I, Mikulskas I, Tomasiunaset R, Muller D, Grob J-J, Rehspringer J-L and Honerlage B 2002 *J. Appl. Phys.* **91** 2896
[60] Fauchet P M and Ruan J 2003 *Towards the First Silicon Laser (NATO Series)* ed L Pavesi, S Gaponenko and L Dal Negro (New York: Kluwer) p 197
[61] Ivanda M, Densica U V, White C W and Kiefer W 2003 *Towards the First Silicon Laser (NATO Series)* ed L Pavesi, S Gaponenko and L Dal Negro (New York: Kluwer) p 191
[62] Dal Negro L, Cazzanelli M, Gaburro Z, Bettotti P, Pavesi L, Priolo F, Franzò G, Pacifici D and Icona F 2003 *Towards the First Silicon Laser (NATO Series vol 93)* ed L Pavesi, S Gaponenko and L Dal Negro (New York: Kluwer) p 145
[63] Valenta J, Pelant I and Linnros J 2002 *Appl. Phys. Lett.* **81** 1396
[64] Icona F, Franzò G, Moreira E C and Priolo F 2001 *J. Appl. Phys.* **89** 8354
[65] An introduction and up-to-date review can be found in Gaburro Z and Pavesi L 2003 Light emitting diodes for Si integrated circuits *Handbook of Luminescence, Display Materials, and Nanocomposites* ed H S Nalwa and L S Rohwer (Stevenson Ranch: American Scientific)
[66] Franzò G, Irreira A, Moreira E C, Miritello M, Icona F, Sanfilippo D, Di Stefano G F, Fallica F and Priolo F 2002 *Appl. Phys.* A **74** 1
[67] Lin Ching-Fuh, Chung Peng-Fei, Chen Miin-Jang and Su Wei-Fang 2002 *Opt. Lett.* **27** 713
[68] Heikkila L, Kuusela T T and Hedman H P 1999 *Superlatt. Microstruct.* **26** 157
[69] Becker P C, Olsson N A and Simpson J R 1999 *Erbium-Doped Fibre Amplifiers* (London: Academic)
[70] Priolo F 1999 *Silicon Based Microphotonics: from Basics to Applications* ed O Bisi, S U Campisano, L Pavesi and F Priolo (Amsterdam: IOS Press) p 279
Polman A 1997 *J. Appl. Phys.* **82** 1
[71] Franzò G, Priolo F, Coffa S, Polman A and Carnera A 1994 *Appl. Phys. Lett.* **64** 2235
[72] Coffa S, Franzò G and Priolo F 1996 *Appl. Phys. Lett.* **69** 2077
[73] Coffa S, Franzò G, Priolo F, Pacelli A and Lacaita A 1998 *Appl. Phys. Lett.* **73** 93
[74] Franzò G, Vinciguerra V and Priolo F 1999 *Appl. Phys.* A **69** 3
Franzo G, Pacifici D, Vincigueraa V, Priolo F and Iacona F 2000 *Appl. Phys. Lett.* **76** 2167
[75] Zacharias M, Heitmann M S J and Streitenberger P 2001 *Physica* E **11** 245
[76] Kik P G and Polman A 2003 *Towards the First Silicon Laser (NATO Series)* ed L Pavesi, S Gaponenko and L Dal Negro (New York: Kluwer) p 383
[77] Zhao X, Komuro S, Isshiki H, Aoyagi Y and Sugano T 1999 *Appl. Phys. Lett.* **74** 120
[78] Han Hak-Seung, Seo Se-Young and Shin Jung H 2001 *Appl. Phys. Lett.* **79** 4568
[79] Priolo F, Franzo G, Pacifici D, Vinciguerra V, Iacona F and Irrera A 2001 *J. Appl. Phys.* **89** 264
[80] Kenyon A J, Chryssou C E, Pitt C W, Shimizu-Iwayama T, Hole D E, Sharma N and Humphreys C J 2002 *J. Appl. Phys.* **91** 367
[81] Kik P G and Polman A 2002 *J. Appl. Phys.* **91** 534
[82] Soref R A 1997 *Thin Solid Films* **294** 325
[83] Gmachl C *et al* 2001 *Rep. Prog. Phys.* **64** 1533
[84] Dehlinger G, Diehl L, Gennser U, Sigg H, Faist J, Ensslin K and Grützmacher D 2000 *Science* **290** 2277
[85] Dehlinger G, Diehl L, Gennser U, Sigg H, Muller E, Stutz S, Faist J, Stangl J, Roch T, Bauer G and Grutzmacher D 2002 *Mater. Sci. Eng.* B **89** 30
[86] Diehl L *et al* 2003 *Towards the First Silicon Laser (NATO Series vol 93)* ed L Pavesi, S Gaponenko and L Dal Negro (New York: Kluwer) p 325
[87] Bormann I, Brunner K, Hackenbuchner S, Zandler G, Abstreiter G, Schmult S and Wegscheider W 2002 *Appl. Phys. Lett.* **80** 2260
[88] Diehl L, Mentese S, Sigg H, Müller E, Grützmacher D, Gennser U, Sagnes I, Fromherz T, Stangl J, Roch T, Bauer G, Campidelli Y, Kermarrec O, Bensahel D and Faist J 2002 *Appl. Phys. Lett.* **81** 4700
[89] Kohler R, Tredicucci A, Beltram F, Beere H, Linfield E, Davies G, Ritchie D, Iotti R C and Rossi F 2002 *Nature* **417** 156
[90] Lynch S A, Bates R, Paul D J, Norris D J, Cullis A G, Ikonic Z, Kelsall R W, Harrison P, Arnone D D and Pidgeon C R 2002 *Appl. Phys. Lett.* **81** 1543

[91] Lynch S A, Dhillon S S, Bates R, Paul D J, Arnone D D, Robbins D J, Ikonic Z, Kelsall R W, Harrison P, Norris D J, Cullis A G, Pidgeon C R, Murzyn P and Loudon A 2002 *Mater. Sci. Eng.* B **89** 10

[92] Kelsall R W, Ikonic Z, Harrison P, Lynch S A, Bates R, Paul D J, Norris D J, Liew S L, Cullis A G, Robbins D J, Murzyn P, Pidgeon C R, Arnone D D and Soref R A 2003 *Towards the First Silicon Laser (NATO Series)* ed L Pavesi, S Gaponenko and L Dal Negro (New York: Kluwer) p 367

[93] Pavlov S G, Hübers H-W, Rümmeli M H, Hovenier J N, Klaasen T O, Zhukavon R Kh, Muravjov A V and Shastin V N 2003 *Towards the First Silicon Laser (NATO Series vol 93)* ed L Pavesi, S Gaponenko and L Dal Negro (New York: Kluwer) p 331

Shastin V N, Orlova E E, Zhukavin R Kh, Pavlov S G, Hübers H-W and Riemann H 2003 *Towards the First Silicon Laser (NATO Series vol 93)* ed L Pavesi, S Gaponenko and L Dal Negro (New York: Kluwer) p 341

[94] Shastin N, Zhukavin R Kh, Orlova E E, Pavlov S G, Rummeli M H, Hubers H-W, Hovenier J N, Klaassen T O, Riemann H, Bradley I V and van der Meer A F G 2002 *Appl. Phys. Lett.* **80** 3512

[95] Blom A, Odnoblyudov M A, Cheng H H, Yassievich I N and Chao K A 2001 *Appl. Phys. Lett.* **79** 713

[96] Pavlov S G, Zhukavin R Kh, Orlova E E, Shastin V N, Kirsanov A V, Hubers H-W, Auen K and Riemann H 2000 *Phys. Rev. Lett.* **84** 5220

Pavlov S G, Hubers H-W, Riemann H, Zhukavin R Kh, Orlova E E and Shastin V N 2002 *J. Appl. Phys.* **92** 5632

[97] Ascombe N 2003 Seeking a silicon laser *Photon. Spectra* **February** 62

[98] Soref R A 1999 *Silicon Based Microphotonics: from Basics to Applications* ed O Bisi, S U Campisano, L Pavesi and F Priolo (Amsterdam: IOS Press) p 1